treatment in wetlands; it uses variables such as geometric storage shape, inflow and outflow rates, and influent and effluent concentrations. One of the models used in modeling both systems is the k-C^* model. The model has been applied to constructed wetland performance, which has resulted in good reproducibility of real situations (Kadlec 2000, 2003; Rousseau et al. 2004, Stone et al. 2004). It incorporates "irreducible minimum concentration" to the first-decay equation, where the observed effluent concentration converges to a constant value. Assumptions of steady-state and plug flow conditions, typical of flow hydrodynamics within wetland systems (Kadlec and Knight 1996), are adopted. The model is defined by

$$C_{out} = C^* + (C_{in} - C^*)e^{-k/q} \tag{9-42}$$

where

C_{in} and C_{out} = influent and effluent event mean concentration (EMC) (mg/l),
C^* = background EMC or irreducible minimum concentration (mg/l),
k = aerial removal rate constant (m/day),
$q = Q/A_{BMP}$ = BMP hydraulic loading rate (m/day),
Q = average inflow rate (m^3/day), and
A_{BMP} = surface area of the BMP (m^2).

Although the model assumes steady-state flow conditions, the BMP fills quickly and drains over a long period (24 to 72 h) at an essentially constant rate. For that reason, the assumption is reasonable for BMPs. The k-C^* model has been used to model wetland performance, and many studies have verified that this model characterizes the removal of pollutants by wetlands very well (Kadlec and Knight 1996; Kadlec 2000, 2003; Braskerud 2002; Rousseau et al. 2004; Lin et al. 2005). Wong et al. (2002, 2006) and Huber et al. (2006) use the k-C^* model to simulate stormwater BMPs because the characteristics of wetlands, detention basins and retention ponds are similar.

Uncertainty in the BMP performance to be discussed here includes (1) the uncertainty in the input pollutant concentration of the runoff, C_{in}, which can be calculated using a log–normal distribution of EMC from field data or literature, and (2) the uncertainty in BMP treatment effectiveness, which is accounted for by associating the uncertainty with the key performance parameters of the k-C^* model.

9.2.2.1 Uncertainty of C_{in}

BMP performance data from the International Stormwater BMP Database (www.bmpdatabase.org) maintained by ASCE and the US Environmental Protection Agency (USEPA) can be used for characterizing uncertainty in C_{in}. For example, Table 9-4 lists the locations, number of datasets, and

Table 9-4. Examples of Detention Basins.

		BMP size			
BMP type	*BMP name, location*	*Number of datasets*	*Volume (m^3)*	*Surface area (ha)*	*Length (m)*
Detention basin	15/78, Escondido, CA	17	1,122.54	0.0977	60.96
	5/605 EDB, Downey, CA	2	364.66	0.0598	47.24
	605/91 edb, Cerritos, CA	5	69.57	0.0114	22.86
	Manchester, Encinitas, CA	12	252.79	0.0304	22.86

Source: Park et al. (2011).

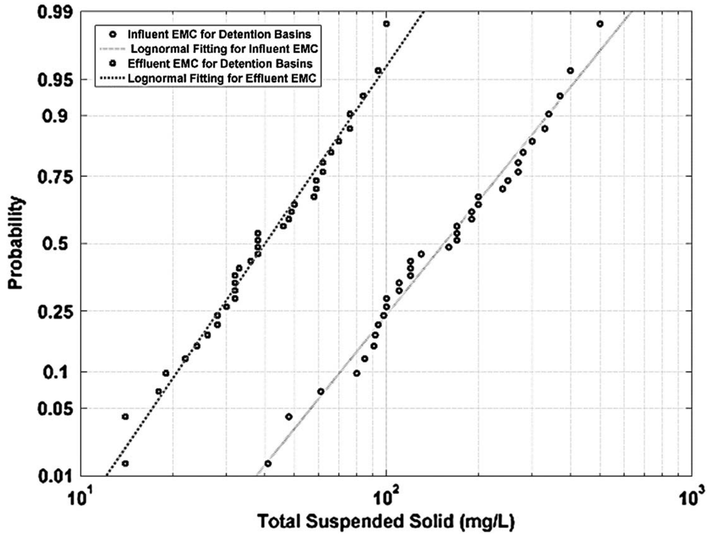

Figure 9-6. Log–normal probability plots of observed C_{in} and C_{out} in detention basins.
Source: Park et al. (2011).

Table 9-5. Results of Goodness-of-Fit Tests; Observed C_{in} and C_{out} from Figure 9-6.

	Critical value (α = 0.10)		
Test	C_{in}	C_{out}	*Decision*
Chi–square	0.663	0.860	Accept
Kolmogorov–Smirnov	0.789	0.852	Accept
Anderson–Darling	0.567	0.685	Accept

Source: Park et al. (2011).

sizes of four dry detention BMPs for retrieved total suspended solids (TSS) data, a representative nonpoint-source pollutant. TSS distributions for both C_{in} and C_{out} in these locations are well represented as log–normal probability plots (Figure 9-6). Table 9-5 shows the results of three goodness-of-fit tests using the well-known chi–squared, Kolmogorov–Smirnov, and Anderson–Darling tests. To apply these tests for normality, all C_{in} and C_{out} values were transformed using the natural logarithm (D'Agostino and Stephens 1986, Kottegoda and Rosso 1997). All tests at a significance level of 0.1 showed that a log–normal distribution can be accepted for both observed C_{in} and observed C_{out}.

9.2.2.2 Uncertainty of Parameter k

The parameter k is related to q with a power function in the k-C^* model (Schierup et al. 1990, Lin et al. 2005). However, the variance of C_{out}, simulated with the k-C^* model, changes dramatically depending on k. Therefore, applying a prediction interval in the k versus q regression line is necessary. A prediction interval focuses on the variance of individual data, whereas a confidence interval focuses on the variance of a regression line. The prediction is calculated as (Kutner et al. 2004)

$$Mean \pm t_{0.025}s\sqrt{1+\frac{1}{n}+\frac{(X-\overline{X})^2}{\sum_{i=1}^{n}(X_i-\overline{X})^2}} \qquad (9\text{-}43)$$

where

t = critical value of the t distribution for the appropriate degree of freedom $(n-2)$,
n = number of total data,
s = standard error of the regression,
X = average q at which the confidence interval is calculated,
$\overline{X}$ = mean of observed q from monitoring data, and
X_i = individual observed q from monitoring data.

For TSS in BMPs, Figure 9-7 exhibits a power regression relation given by $k = 1.4841q^{0.9721}$, similar to the ones identified by Schierup et al. (1990) and Lin et al. (2005). A regression of estimated k using Equation (9-42) versus observed q for each storm event was performed with a 95% prediction interval of 0.4370. Then, the vertical distribution generating k depending on q is considered a two-parameter log–normal distribution.

9.2.2.3 Estimation of C^*

This approach assumes a known constant value of C^* because its uncertainty is less relevant than the uncertainty of C_{in} or k. This also helps with reducing the number of parameters needed in the uncertainty analysis. From the minimum C_{out} in the dataset and the range of C^* suggested in the literature (Table 9-6), we choose a value of $C^* = 10$ mg/L.

What follows is the uncertainty analysis considering three cases, which require specific information (Table 9-7): uncertainty in C_{in}, uncertainty in k, and uncertainty in both. For example,

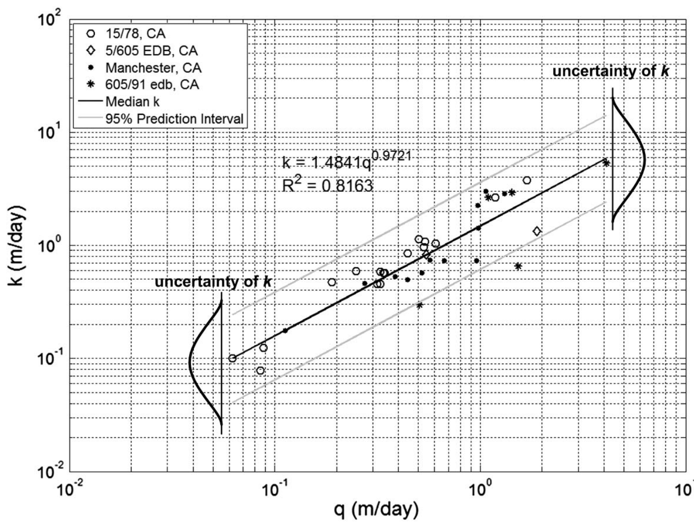

Figure 9-7. Estimated k *versus* q *using individual storm events for detention basins.*
Source: Park et al. (2011).

Table 9-6. Typical Background Concentration Values Proposed in Literature.

Literature	*TSS (mg/L)*
Kadlec and Knight (1996)	$5.1 + 0.16\ C_{in}$
Barrett (2004)	$5 \sim 20$
Crites et al. (2006)	6

Source: Park et al. (2011).

Table 9-7. Required Parameters Information of C_{in} and k for Uncertainty Analyses.

Input parameters		C_{in}		K	
Log–transformed statistical properties		*Mean = 5.038*	*Std. dev. = 0.6083*	*Mean = log (1.4841q$^{0.9721}$)*	*Std. dev. = 0.437*
Uncertainty in	C_{in}	✓	✓	✓	–
	k (with constant C_{in})	✓	–	✓	✓
	k (with constant q)	✓	–	✓	✓
	C_{in} and k	✓	✓	✓	✓

Source: Park et al. (2011).
✓ = required information for uncertainty computation.

to analyze the uncertainty in C_{in}, the required information is the log–transformed standard deviation of C_{in} and the log–transformed means of C_{in} and k. The standard deviation of k can be estimated from the distance of the prediction interval between the median k and the 95% prediction interval shown in Figure 9-7.

9.2.3 Methods for Uncertainty Analysis

Three methods, the derived distribution method (DDM) for the analytical method, the first-order second moment (FOSM) for the approximation method, and the Latin hypercube sampling (LHS) for the Monte Carlo simulation, are applied for estimating uncertainty of C_{out} in the k-C^* model.

9.2.3.1 Derived Distribution Method

In the DDM, the PDF of a variable $Y = g(X)$ can be obtained given the PDF of X, $f_x(x)$. The transformation from the PDF of X to that of Y entails the substitution of the inverse function of Y solved for X in the PDF of X. Then, the PDF of Y is (Salas et al. 2004)

$$f_Y(Y) = \left|\frac{dg^{-1}(Y)}{dy}\right| f_x[g^{-1}(Y)] \tag{9-44}$$

In our case, the variable Y is C_{out}, and the variable X would be either C_{in} or k.

9.2.3.2 First-Order Second Moment

In cases where analytical methods such as DDM are cumbersome to apply, approximate methods have been suggested. For example, FOSM uses a Taylor-series expansion of the performance function and enables estimating the mean and variance of the performance function as

$$E(Y) = E[g(X_1, \cdots, X_n)] \approx g(\mu_1, \cdots, \mu_n) \tag{9-45}$$

$$Var(Y) = Var[g(X_1, \cdots, X_n)] \approx \sum_{j=1}^{n} \left(\frac{\partial g}{\partial X_i}\right)_{\mu}^{2} Var(X_i) + \sum_{i=1}^{n}\sum_{j=1}^{n} \left(\frac{\partial g}{\partial X_i}\right)_{\mu} \left(\frac{\partial g}{\partial X_j}\right)_{\mu} Cov(X_i, X_j) \tag{9-46}$$

Assuming that the X_i's are independent variables, $Cov(X_i, X_j) = 0$. Then the variance of Y is

$$Var(Y) = Var[g(X_1, \cdots, X_n)] \approx \sum_{j=1}^{n} \left(\frac{\partial g}{\partial X_i}\right)_{\mu}^{2} Var(X_i) \tag{9-47}$$

where $\hat{\mu}_{\ln x}$ and $\hat{\sigma}_{\ln x}$ can be calculated from the sample mean and standard deviation of log–transformed X. Finally, the inverse of the CDF is calculated to quantify the percentile of the log–normal distribution using the estimated parameters (Salas et al. 2004):

$$X_p = \exp(\mu_{\ln x} \pm Z\sigma_{\ln x}) \tag{9-48}$$

where Z is the standard normal quantile corresponding to exceedance probability, and X_p is the X value of p percentile.

9.2.3.3 Latin Hypercube Sampling

LHS is a stratified sampling method to reduce variance and sampling error. The steps to apply the method are as follows (Tung and Yen 2005):

1. Select the number of subintervals, L, and divide the range [0, 1] into L equal intervals.
2. For each subinterval, define ω_i as independent-uniform-random numbers from $\omega_l \sim U\left(\frac{0,1}{L}\right)$ for $l = 1, 2, \ldots, L$. Then, a sequence of probability values u_m is generated as
   a. $u_i = \frac{l-1}{L} + \omega_l \quad l = 1, 2, \ldots, L$
3. Compute $Z_l = F^{-1}(u_l)$, in which $F(\cdot)$ is the CDF of the random variable of standard normal distribution.
4. Compute mean and standard deviation from log–transformed C_{in} or k.
5. Compute generated C_{in} or k assuming log–normal distribution as $X_l = \exp(\mu_{lnx} + Z_l\sigma_{lnx})$.
6. Apply generated C_{in} or k to the k-C^* model.

9.2.4 Sensitivity Results

The distribution of C_{out} for the k-C^* model is then estimated with the two identified distributed input parameters, C_{in} and k. Results of uncertainty in C_{in}, uncertainty in k, and uncertainty in both C_{in} and k can be computed. These results assume that geometric (A_{BMP}) and hydrological parameters (Q) don't have uncertainty. In addition, the background concentration (C^*) is fixed at 10 mg/L because the minimum value of the observed data used was close to that concentration. C_{in} and k were represented as log–normal distributions because their observed distributions are very close to log–normal (Figure 9-6).

9.2.4.1 Sensitivity of Uncertainty in C_{in}

The following log–normal distribution $f_{C_{in}}(C_{in})$ for C_{in} is assumed with a mean value $\mu_{LnC_{in}}$ and standard deviation $\sigma_{LnC_{in}}$ from the selected TSS of detention basins in the BMP database (see also Figure 9-6):

$$f_{C_{in}}(C_{in}) = \frac{1}{\sqrt{2\pi} C_{in} \sigma_{lnC_{in}}} \exp\left[-\frac{1}{2}\left(\frac{\ln(C_{in}) - \mu_{lnC_{in}}}{\sigma_{lnC_{in}}}\right)^2\right] \tag{9-49}$$

According to Equation (9-44), the PDF for C_{out}, $f(C_{out})$ is given by

$$f_{C_{out}}(C_{out}) = \left| \frac{dg^{-1}(C_{out})}{dC_{out}} \right| f_{c_{in}}[g^{-1}(C_{out})] \tag{9-50}$$

where,

$$g^{-1}(C_{out}) = C^* + (C_{out} - C^*)\exp(k/q) = C_{in} \tag{9-51}$$

$$\left| \frac{dg^{-1}(C_{out})}{dC_{out}} \right| = |\exp(k/q)| = \exp(k/q) \tag{9-52}$$

Substituting Equation (9-51) and Equation (9-52) into Equation (9-50), the resulting PDF for the effluent EMC, $f_{out}(C_{out})$, is

$$f(C_{out}) = \frac{1}{\sqrt{2\pi}\left[C_{out} - C^*\left\{1 - \frac{1}{\exp\left(\frac{k}{q}\right)}\right\}\right]\sigma_{lnC_{in}}} \exp\left[-0.5\left(\frac{\ln\left[C_{out} - C^*\left\{1 - \frac{1}{\exp\left(\frac{k}{q}\right)}\right\}\right] - \left(\mu_{lnC_{in}} - \left(\frac{k}{q}\right)\right)}{\sigma_{lnC_{in}}}\right)^2\right] \tag{9-53}$$

Adopting the relationship $k = 1.4841q^{0.9721}$ (Figure 9-8), we obtain

$$f(C_{out}) = \frac{1}{\sqrt{2\pi}\left[C_{out} - C^*\left\{1 - \frac{1}{\exp(1.481q^{-0.0279})}\right\}\right]\sigma_{lnC_{in}}} \exp\left[-0.5\left(\frac{\ln\left[C_{out} - C^*\left\{1 - 1 - \frac{1}{\exp(1.481q^{-0.0279})}\right\}\right] - \left(\mu_{lnC_{in}} - 1.4841q^{-0.0279}\right)}{\sigma_{lnC_{in}}}\right)^2\right] \tag{9-54}$$

Equation (9-54) shows that $f(C_{out})$ is a three-parameter log–normal distribution, whose scale parameter $(1.481q^{-0.0279})$ and location parameter $(C^*\{1 - 1/\exp(1.481q^{-0.0279})\})$ vary with q. $f(C_{out})$ is very sensitive to the value of $\exp(1.481q^{-0.0279})$ when it is a function of q and becomes closer to the two-parameter log–normal distribution as $\exp(1.481q^{-0.0279})$ approximates to 1. However, $f(C_{out})$ changes to the three-parameter log–normal distribution for values of $\exp(1.481q^{-0.0279})$ much greater than 1.

Figure 9-8a shows comparisons of the PDFs for the three methods: DDM, LHS, and FOSM. DDM is derived from Equation (9-54) with constant q. C_{out} assumes a two-parameter log–normal distribution. The PDF obtained using FOSM differs from the DDM and the LHS when q is both 0.01 and 5 m/day. Conceptual differences among the three methods explain this discrepancy. No assumptions regarding the distribution of C_{out} are required by DDM and LHS methods. In contrast, a known PDF must be assumed for C_{out} when using the FOSM method. This assumption makes the method simpler but introduces error. DDM is the most accurate method, but defining the exact value corresponding to a specific percentile is difficult because an extra computation is needed to estimate the percentile from the PDF matched with C_{out}. With LHS, estimating the precise value of a specific percentile is relatively easy.

For $q = 0.01$ and 5 m/day, $\exp(1.481q^{-0.0279})$ is 5.41 and 4.13, respectively. Both values are much greater than 1, and the PDF in Equation (9-54) differs from the log–normal distribution to a large extent. This creates the differences observed between the DDM and LHS PDFs and the log–normal PDF obtained using FOSM. Thus, LHS gives the correct representation rather than FOSM because the LHS PDFs coincide with the DDM PDFs.

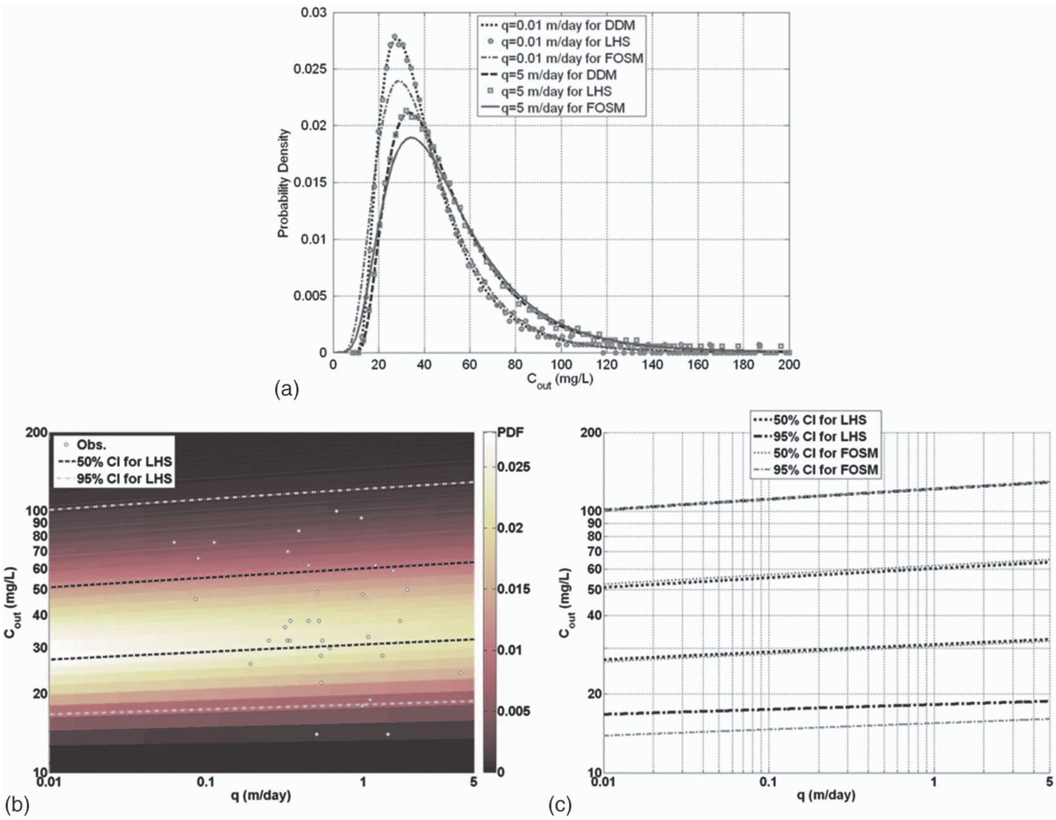

Figure 9-8. Uncertainty in C_{in}*: (a) PDFs comparison of* $f(C_{out})$ *among DDM, LHS, and FOSM; (b) PDFs of LHS, including confidence intervals (CIs) and observed data; and (c) comparison of CIs between LHS and FOSM.*
Source: Park et al. (2011).

The obtained PDFs of C_{out} represent the observed data well (Figure 9-8b). The 95% and 50% confidence intervals represent the high variability of the data, with C_{out} values being higher and more scattered for large values of q. Most of the observed data are low q values. As expected, about half of the observed data are placed out of the 50% confidence interval and two points (5% of the total data) are located outside of the 95% confidence interval. Figure 9-8c compares the 50% and 95% upper and lower confidence intervals obtained using LHS and FOSM. With the exemption of the lower 95% confidence limits, the rest of the limits are very similar. Hence, the distributed C_{out} is essentially identical for LHS and FOSM.

9.2.4.2 *Sensitivity of Uncertainty in* k *with Constant* q

A constant value of q must be adopted to determine the effect of C_{in} on the uncertainty of C_{out} with respect to k. In this case, we use $q = 0.1$ m/day. The mean and standard deviation of the log-transformed k are obtained from Table 9-7. The uncertainty in k with constant C_{in} for DDM can be simplified as follows:

$$f(C_{out}) = \frac{1}{\sqrt{2\pi} ln\left(\frac{C_{in}-C^*}{C_{out}-C_*}\right)\sigma_{lnk}\left|(C_{out}-C^*)\right|}\exp\left[-\frac{1}{2}\left(\frac{\ln\left[0.1\ln\left(\frac{C_{in}-C^*}{C_{out}-C_*}\right)\right]-\mu_{lnk}}{\sigma_{lnk}}\right)^2\right] \tag{9-55}$$

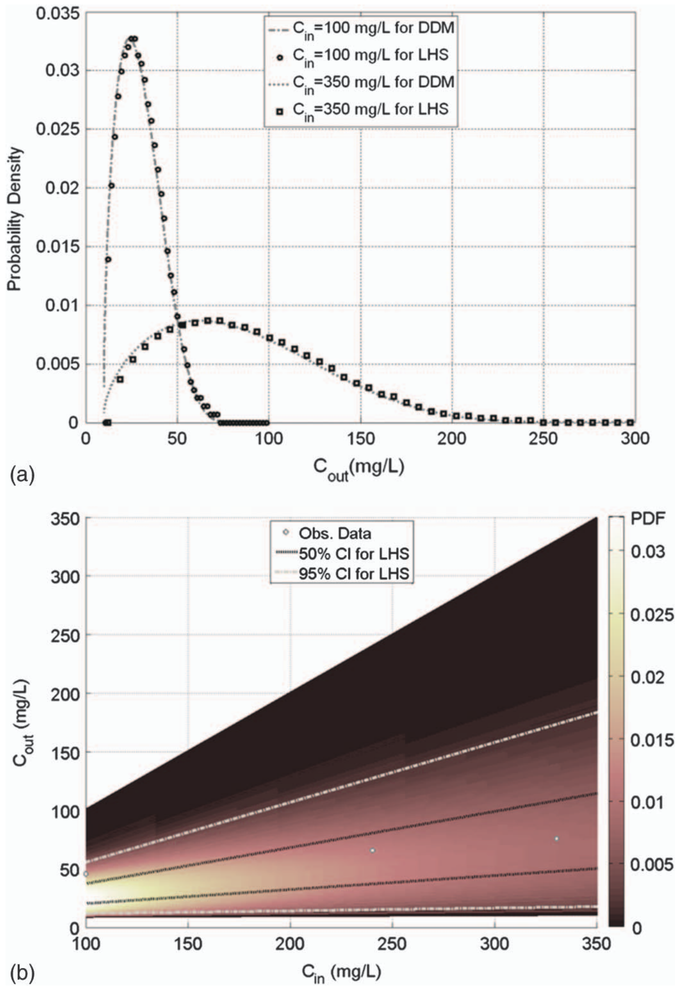

Figure 9-9. Uncertainty in k *with constant* q*: (a) PDFs comparison of* $f(C_{out})$ *as a function of* C_{in} *using* q *= 0.1 m/day between DDM and LHS and (b) PDFs from LHS, including confidence intervals (CIs) and observed data.*

Source: Park et al. (2011).

Figure 9-9a shows both PDFs for values of C_{in} = 100 mg/L and 350 mg/L. In this case, only DDM and LHS are used for the uncertainty analysis. FOSM cannot be used because the C_{out} distribution of Equation (9-55) is difficult to define. Both methods produce very similar distributions and represent a higher variability in C_{out} as C_{in} increases. In other words, predicting C_{out} is more difficult for a high C_{in} at a constant q. Figure 9-9b shows the PDFs of C_{out} for the observed data when q is restricted to 0.1 m/day. This figure shows the PDF computed using LHS, but almost identical results are obtained with the PDFs using DDM, as Figure 9-9a illustrates. The 95% and 50% confidence intervals become wider as q increases. For this analysis, only three observed data points from Table 9-7 were available as q = 0.1 m/day; two of the three points lie within the 50% confidence interval and the third is within the 95% confidence interval.

9.2.4.3 Sensitivity of Uncertainty in k *with Constant* C_{in}

A constant value of C_{in} = 170 mg/L is assumed to determine the effect of q on the uncertainty of k. In this case, the mean and standard deviation of log-transformed k are obtained from Table 9-7. Figure 9-10a shows PDFs for values of q = 0.01 m/day and 5 m/day. Then, the DDM is given by

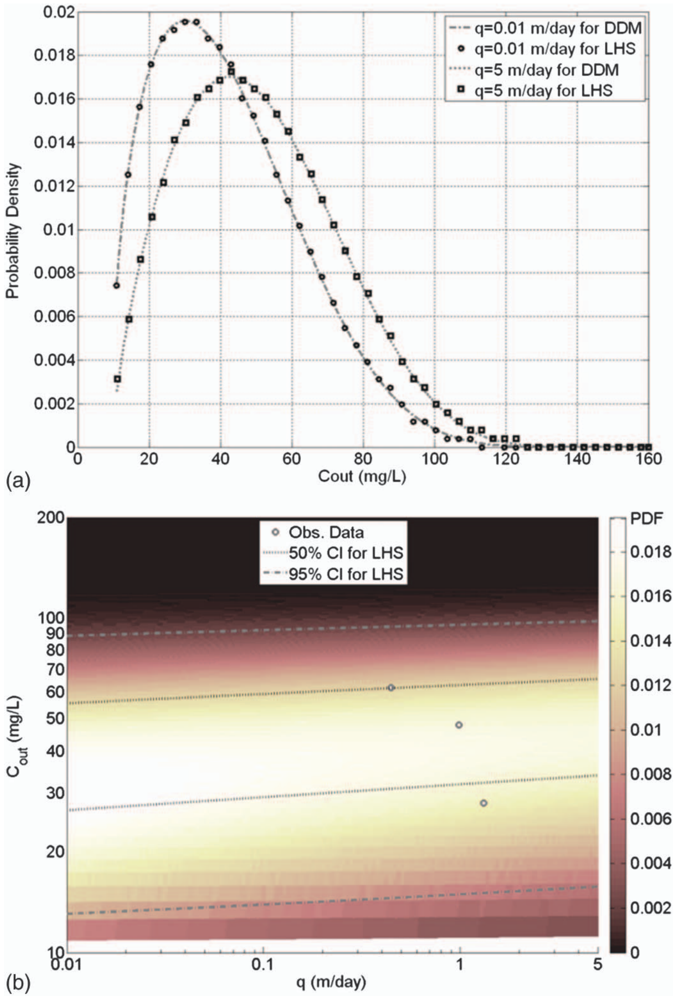

Figure 9-10. Uncertainty in k with constant C_{in}: (a) comparison of $f(C_{out})$ as a function of q using C_{in} = 170 mg/L between DDM and LHS and (b) PDFs from LHS, including confidence intervals (CIs) and observed data.
Source: Park et al. (2011).

$$f(C_{out}) = \frac{1}{\sqrt{2\pi} ln\left(\frac{170-C^*}{C_{out}-C^*}\right)\sigma_{lnk}|(C_{out}-C^*)|}\exp\left[-\frac{1}{2}\left(\frac{ln\left[q\, ln\left(\frac{170-C^*}{C_{out}-C^*}\right)\right]-\mu_{lnk}}{\sigma_{lnk}}\right)^2\right] \quad (9\text{-}56)$$

Again, we use only DDM and LHS for the uncertainty analysis for the same reason given in the previous subsection. Both the DDM and LHS methods produce very similar distributions and represent higher variability in C_{out} as q increases. In other words, the shapes of the PDFs of C_{out} demonstrate a more positive skew with decreasing q. As a result, predict C_{out} for high q is more difficult at a constant C_{in}.

Figure 9-10b shows PDFs of C_{out} for the observed data obtained from Table 9-4 when C_{in} is restricted to 170 mg/L. The 95% and 50% confidence intervals are plotted as well. These intervals indicate that C_{out} values are higher and a little more scattered for larger values of q. Two of the three observed datasets are scattered within the 50% confidence interval, and a third point is located within the 95% confidence interval. Although having only three datasets available for comparison, they do validate that PDFs of the k-C^* model describe the behavior of observed data. Based on the previous results, the shape of the PDF as a function of C_{in} was found to show more change of variance than as a function of q. It can be concluded that C_{in} is a more sensitive variable than q for the uncertainty in k when the k-C^* model is considered with TSS.

9.2.4.4 Sensitivity in Both C_{in} *and* k

This section assumes no correlation between C_{in} and k to simplify the calculations. Because of mathematical complexities, the DDM cannot be applied to derive $f(C_{out})$ when uncertainties in both C_{in} and k are simultaneously applied to the k-C^* model. Thus, we use the FOSM method and the LHS method, which have been shown to generate similar distributions as the DDM method.

Figure 9-11a shows a comparison of both PDFs for $q = 0.01$ and $q = 5$ m/day. Both distributions are relatively similar for $q = 5$ m/day, but differences are observed in the peak values for $q = 0.01$ m/day. The distribution of C_{out} is skewed to the right for both values of q. As mentioned previously, the FOSM assumes a log–normal distribution. Thus, the shapes of the PDFs generated by the LHS and FOSM methods are expected to differ. Figure 9-11b shows the PDFs obtained with LHS, their confidence intervals of 50% and 95%, and the observed data. About two-thirds of the total data

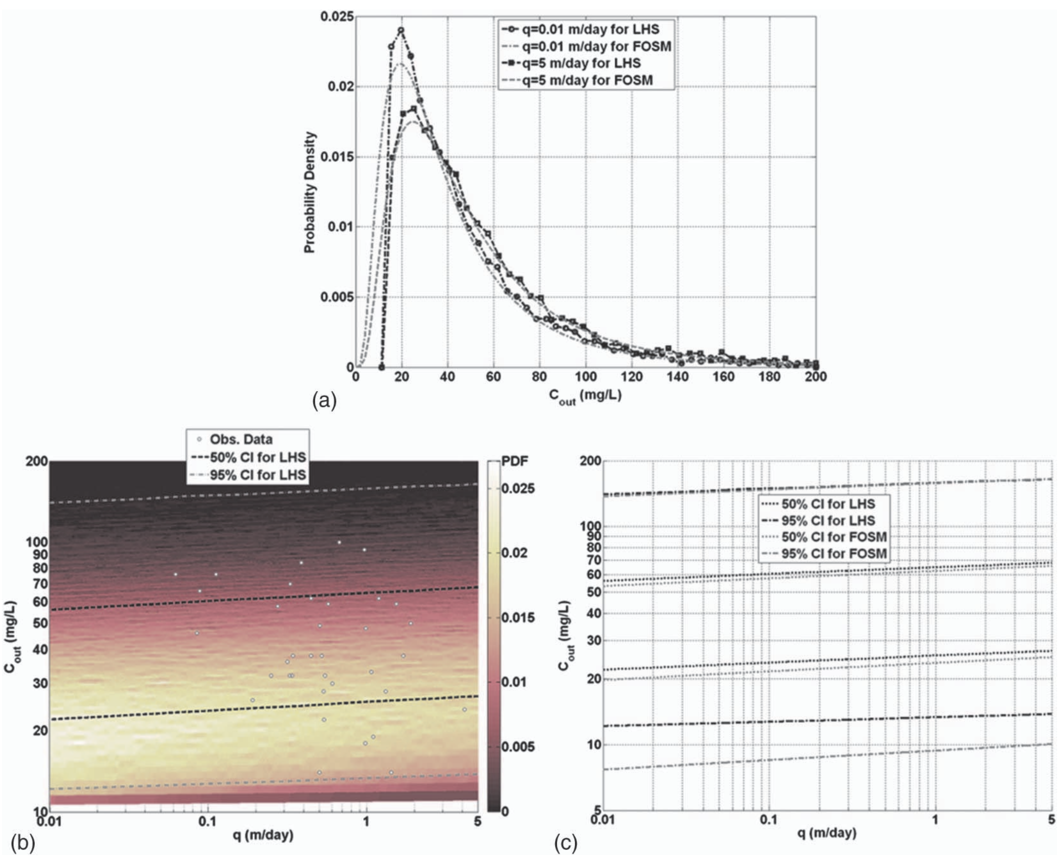

Figure 9-11. Uncertainty in both C_{in} *and* q*: (a) PDFs comparison of* $f(C_{out})$ *as a function of* q *between LHS and FOSM; (b) PDFs from LHS, including confidence intervals (CIs) and observed data; and (c) comparison of CIs between LHS and FOSM.*
Source: Park et al. (2011).